Improvement of the Richardson-Zaki liquid-solid fluidisation model on the basis of hydraulics

Kramer, Onno; de Moel, Peter; Baars, E.T.; van Vugt, W.H.; Padding, Johan; van der Hoek, Jan Peter

DOI
10.1016/j.powtec.2018.11.018

Publication date
2019

Document Version
Final published version

Published in
Powder Technology

Powder Technology 343 (2019) 465–478

Contents lists available at ScienceDirect

Powder Technology

journal homepage: www.elsevier.com/locate/powtec

Improvement of the Richardson-Zaki liquid-solid fluidisation model on the basis of hydraulics

O.J.I. Kramer [a,b,c,d,*], P.J. de Moel [a,e], E.T. Baars [c], W.H. van Vugt [d], J.T. Padding [b], J.P. van der Hoek [a,c]

[a] Delft University of Technology, Faculty of Civil Engineering and Geosciences, Department of Water Management, PO Box 5048, 2600, GA, Delft, the Netherlands
[b] Delft University of Technology, Faculty of Mechanical, Maritime and Materials Engineering, Department of Process and Energy, Leeghwaterstraat 39, 2628, CB, Delft, the Netherlands
[c] Waternet, PO Box 94370, 1090, GJ, Amsterdam, the Netherlands
[d] HU University of Applied Sciences Utrecht, Institute for Life Science and Chemistry, PO Box 12011, 3501, AA, Utrecht, the Netherlands
[e] Omnisys, Eiberlaan 23, 3871, TG, Hoevelaken, the Netherlands

ARTICLE INFO

Article history:
Received 17 July 2018
Received in revised form 25 September 2018
Accepted 3 November 2018
Available online 06 November 2018

Keywords:
Liquid-solid fluidisation
Drinking water
Richardson-Zaki
Minimal fluidisation
Terminal settling velocity
Hydraulic models

ABSTRACT

One of the most popular and frequently used models for describing homogeneous liquid-solid fluidised suspensions is the model developed by Richardson & Zaki in 1954. The superficial fluid velocity and terminal settling velocity together with an index makes it possible to determine the fluid porosity in a straightforward way. The reference point for the Richardson-Zaki model is the terminal settling velocity at maximum porosity conditions. To be able to predict porosity in the proximity of minimum fluidisation conditions, either the minimum fluidisation velocity must be known or the Richardson-Zaki index must be very accurate. To maintain optimal process and control conditions in multiphase drinking water treatment processes, the porosity is kept relatively low. Unfortunately, the Richardson-Zaki index models tends to overestimate the minimum fluidisation velocity and therefore also results in less accurate predictions with respect to porosity values. We extended the Richardson-Zaki model with proven hydraulics-based models. The minimum fluidisation velocity is acquired using the model proposed by Kozeny (1927), Ergun (1952) and Carman (1937). The terminal settling velocity is obtained through the model developed by Brown & Lawler (2003), which is an improved version of the well-known model developed by Schiller & Naumann (1933). The proposed models are compared with data from expansion experiments with calcium carbonate grains, crushed calcite and garnet grains applied in drinking water softening using the fluidised bed process. With respect to porosity, prediction accuracy is improved, with the average relative error decreasing from 15% to 3% when the classic Richardson-Zaki model is extended with these hydraulics-based models. With respect to minimum fluidisation velocity, the average relative error decreases from 100% to 12%. In addition, simplified analytical equations are given for a straightforward estimation of the index n.

1. Introduction

The accurate calculation of porosity in water is of major importance in drinking water treatment processes because it determines the process conditions and treatment results. Examples include pellet-softening in fluidised bed reactors [1], sedimentation, flotation and flocculation, filtration processes [2], backwashing of filter media and washing columns in which fine material and impurities are separated from seeding material. In these processes, particle size mostly varies between 0.3 - 2.0 mm, and particle density between 2.5 - 4.0 kg/L. This study focusses on calcium carbonate particles applied in pellet-softening reactors. The softening process involves the dosing of caustic soda, soda ash or lime in a cylindrical up-flow fluidised-bed reactor, which leads to an alteration of the calcium carbonate equilibrium in which the solubility product is exceeded. The reactor is filled with seeding material such as garnet grains (Fig. 1A) or crystal sand grains and pellets. The large specific surface area in the reactor causes the $CaCO_3$ to crystallise on the particles, called pellets (Fig. 1B), as a result of which these grow in size and become increasingly round. If there is no difference in specific density, larger particles will migrate to the lower region of the reactor bed, and a stratified bed will evolve. To retain fluidisation conditions, it is important that the largest pellets, usually those that are larger than 1–2 mm, are extracted from the reactor. These pellets can be used as a by-product in other processes, for instance in industrial and agricultural processes, or they can be re-used as seeding material.

Pellet-softening in a fluidised bed reactor was developed and introduced in the Netherlands in the late 1980s, and by the end of 2018 almost all Dutch drinking water was softened with the help of this technique [3]. For >30 years, crystal sand and garnet grains have been used as seeding material [4]. Process optimisation [5] and control [6] has been focussed primarily on garnet pellets.

* Corresponding author.
E-mail address: o.j.i.kramer@tudelft.nl (O.J.I. Kramer).

https://doi.org/10.1016/j.powtec.2018.11.018

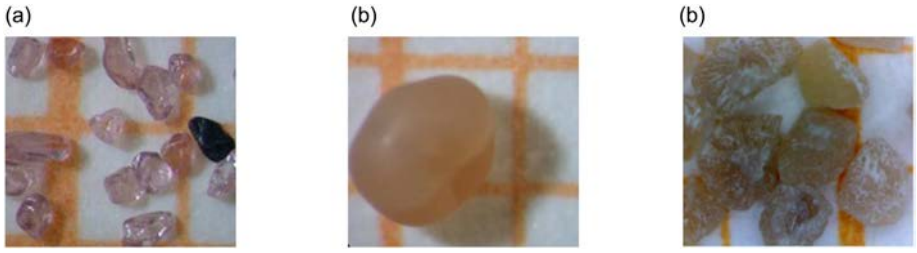

Fig. 1. A) Garnet grains $d_{50} = 0.25$ mm. B) Calcite pellets $d_{50} = 1.05$ mm. C) Crushed calcite pellets $d_{50} = 0.50$ mm.

To meet sustainability goals and to promote the development of a circular economy, water companies have modified their pellet-softening processes, in which garnet grains, mined in Australia, have been replaced by calcite seeding particles that are based on crushed, dried, sieved and re-used calcium carbonate pellets [7]. A second matter to be considered is that the garnet core inside the pellets hinders their potential application in market segments such as the glass, paper, food and feed industries, and it hinders their direct re-use in the pellet reactor itself when it comes to ensuring a more sustainable and circular process. The pellet market value and the sustainability of the softening process can be increased through the substitution of the sand grain by a calcite grain of 0.5 mm (100% calcium carbonate). If the calcite pellets are crushed, dried and sieved, they can be re-used as a seeding material [8]. Due to the crushing of the relatively round pellets, the calcite seeds have an irregular shape (Fig. 1C)[1] and behave differently with respect to settling characteristics in the up-flow fluidisation reactor. In the case of pellet-softening processes using fluidisation, this different sedimentation behaviour can cause unwanted flushing of smaller particles out of the reactor and settling of larger grains to the lower region of the reactor, which leads to a fixed bed state.

To maintain or provide optimal process conditions in pellet-softening reactors, it is important to accurately determine the fluidised bed porosity. Porosity is a crucial variable to determine the specific surface area, the minimum fluidisation and flushing conditions as well as the water and particle residence time. At the bottom of the reactor, the porosity is kept relatively low to obtain the highest crystallisation contact area; nevertheless, fixed bed situations must be avoided. The degree of porosity is dependent on the physical properties of the grains and the water viscosity. De facto, porosity, or fluid bed height, is kept constant through controlling the water flow in the reactor depending on water temperature and through particle bed management. In pellet-softening reactors, porosity is approximately $\varepsilon \approx 0.5$ at the bottom of the reactor and $\varepsilon \approx 0.8$ at the top.

In the literature, several attempts have been made to predict porosity. Asif [9] studied binary solids, and Akgiray & Soyer [10] presented widely used Richardson-Zaki correlations for spherical particles. Slaa et al. [11] showed that the Richardson-Zaki expression underestimates the settling velocities for small particles at high concentrations due to the effect of particle size on the apparent viscosity of the settling silt-water mixture. Đuriš et al. [12] investigated the prediction of bed expansion and minimum fluidisation velocity of sand mixtures in water.

The objective of this paper is to improve the popular Richardson-Zaki model through model enhancement based on hydraulics, which will lead to an improved accuracy of porosity predictions and in particularly for pellet-softening. Through the minimum fluidisation velocity and terminal settling velocity, the Richardson-Zaki index can be calculated accurately. In this way, the index acquires a hydraulic meaning. The numerical prediction of porosity in fluidisation reactors using natural particles with an irregular shape is much more complex than would be the case for perfectly spherical particles. In this work, an improved model is proposed and compared with existing Richardson-Zaki based models, while modelling results are compared with results from a significant number of expansion experiments which were carried out at pilot plant scale. Improved knowledge in this field enables accurate modelling and optimisation for system and control purposes in automated drinking water treatment processes. This is particularly important because unreliable prediction models increase the risk of ineffective treatment processes and higher consumption of chemicals, something which may adversely affect drinking water quality, sustainability goals and costs.

This paper is organised as follows. In Section 2, we give a general overview of the current Richardson-Zaki based models and theory. In Section 3, we discuss the Richardson-Zaki theory applied to the fluidised-bed pellet-softening process and we propose new Richardson-Zaki index equations based on hydraulics. In Section 4, we present our experiments and in Section 5 we show and discuss the results. We end with our conclusions in Section 6.

2. Richardson-Zaki model analyses

2.1. Model principle

A fundamental approach for the description of homogeneously fluidised beds is the well-known and most popular expansion law of Richardson & Zaki, introduced in 1954 [13], which describes the steady state velocity-porosity relationship for sedimenting liquid-solid homogeneous suspensions, but which is also used in gas-solid systems. The model is addressed in a number of standard works: [14–27]. When an ensemble of solid particles is settling in a quiescent liquid, additional hindering effects influence its settling velocity. The drag is increased as a result of the proximity of particles within the ensemble and the up-flow of liquid as it is displaced by the descending particles. According to Richardson & Zaki, the hindering effects are strongly dependent on the porosity ε.

Theoretically, Coulson & Richardson [28], updated in Harker et al. [29], demonstrated that the validity of the Richardson-Zaki equation is limited by the maximum solids concentration that permits solids particle settling in a particulate cloud. This maximum concentration corresponds with the concentration in an incipient fluidised bed or at minimum fluidisation conditions where $\varepsilon = \varepsilon_{mf} \approx 0.4$. In the model, the superficial velocity v_s is linked with particle and fluidised bed characteristics such as the terminal settling velocity v_t of an isolated particle in an unbounded fluid.

$$\varepsilon^n = \frac{v_s}{v_t} \qquad (\varepsilon_{mf} < \varepsilon < 1) \tag{1}$$

Eq. (1) gives a simple relationship between porosity and sedimentation or fluidisation velocity for systems composed of uniform monodispersed spheres dispersed in a liquid. Other expressions which have been proposed in the literature are generally more complex or more limited in their application.

[1] More photographs of particles used in this study can be found in the Supplementary Materials.

2.2. Model boundaries

Theoretically [30], the Richardson-Zaki model intersects two boundary points:

$$\begin{cases} \frac{v_s}{v_t} = 0 & \text{for } \varepsilon = 0 \\ \frac{v_s}{v_t} = 1 & \text{for } \varepsilon = 1 \end{cases} \quad (2)$$

It is known that the index n in the Richardson-Zaki model depends on the flow regime [13]. This influence is visualised in Fig. 2 where the ratio of the superficial and terminal settling velocity is plotted against the porosity. For viscous flow using the classic Stokes particle drag equation, the Richardson-Zaki index tends to $n \rightarrow 4.8$; in the inertial regime, the Richardson-Zaki index tends to $n \rightarrow 2.4$.

Usually, the porosity is considered to be the dependent variable and the superficial velocity the independent variable [18]. Therefore, Fig. 2 displays the superficial velocity on the X-axis and the porosity on the Y-axis. The degree of curvature is determined by the index n, as can be seen in Fig. 2. Deviations in particle size and shape affect the Richardson-Zaki index, which leads to more inaccurate porosity predictions.

In fact, the Richardson-Zaki model does not consider the incipient fluidisation condition. In the vicinity of minimum fluidisation v_{mf}, small deviations in n cause large deviations in the prediction of the minimum fluidisation point when merely the classic Richardson-Zaki model is used (following the curves from v_t to v_{mf} in Fig. 2). Indeed, large deviations in n were already observed in Figs. 5 and 6 included in the article by Khan & Richardson [31]. The most obvious and known points are the inherent terminal settling velocity and the minimum fluidisation velocity. Using these two points, besides the origin (0,0), the index is in fact determined, as we will show in this paper.

2.3. The Richardson-Zaki index n

2.3.1. Popular index equations

In the literature, a collection of equations is given to estimate the Richardson-Zaki index n of which the most popular are presented in Table 1. These equations are based on the single particle Reynolds number Re_t under terminal settling conditions or the Archimedes number Ar.

$$Re_t = \frac{\rho_f d_p v_t}{\eta} \quad (3)$$

$$Ar = \frac{g {d_p}^3 \rho_f \left(\rho_p - \rho_f\right)}{\eta^2} \quad (4)$$

2.3.2. Equation index boundaries

As early as 1949, Lewis et al. [37] found that if the particle is settling under conditions where Stokes' law is valid, n has a value of about 4.65. According to [18,20,36] and others, the Richardson-Zaki index is bounded between the viscous ($n = 4.8$) and the inertial regime ($n = 2.4$). According to [38,39], the value of n lies between 2.4 and 4.6, or between 2.3 and 4.6, respectively, for a wide range of terminal Reynolds numbers.

2.3.3. Alternative index equations

A different empirical equation was proposed by Garside & Al-Dibouni [34]. Rowe [35] gave a convenient empirical equation to estimate the Richardson-Zaki index covering the whole Reynolds range: n_L and n_T are the asymptotic values of n at low and high values of Re_t, respectively, while the position and rate of increase of n in the intermediate region are determined by the coefficients α and β. According to Khan & Richardson, Eq. (7) given by Rowe is an empirical expression which satisfactorily represents the experimental data for n when the effect of the vessel walls is negligible.

Eq. (7) cannot be applied for a given liquid-solid system without prior knowledge of Re_t. Therefore, Khan & Richardson [31] proposed the same form of equation while using the Archimedes number (Eq. (4)) instead of the Reynolds terminal number, albeit with different values of the coefficients α and β.

The Richardson-Zaki model originally included wall effect corrections in Eq. (5). In some works, the wall effect corrections are ignored [5,26,40–42]. Siwiec [33] presented different values of the coefficients c_1 and c_2 for several types of grain materials.

Di Felice [43] and Khan & Richardson [31] presented an overview of existing empirical equations to calculate the Richardson-Zaki index. A collection of improved equations to calculate the index equation was given by Dharmarajah [15] and Akgiray & Soyer [10]. Extension and adjustments of the Richardson–Zaki equation to suspensions of multisided irregular particles were examined by Bargieł & Tory [44], for small fines by Schiaffino & Kytömaa [45], and the expansion behaviour within fixed packings by Glasserman et al. [46]. The relation between the Richardson-Zaki equation and the apparent drag force has been studied by Yang & Renken [47], Valverde & Castellanos [48] and Di Felice [41], and in addition new equations have been proposed for the intermediate regime. The latest proposal was made by Pal & Ghoshal [42], albeit with a different approach, to predict the settling velocity of a sedimenting particle which is dispersed in a sediment-fluid mixture during a turbulent flow. Although theoretically the value of n is restricted between 2.4

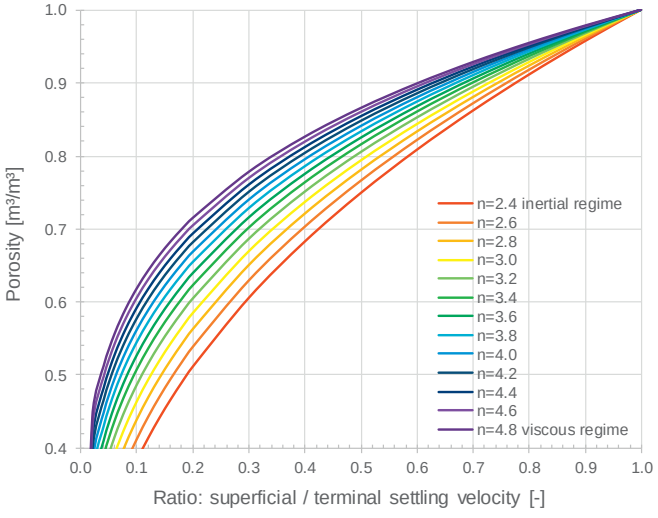

Fig. 2. Richardson-Zaki gradients for various Richardson-Zaki index. The curves are bounded to incipient fluidisation $\varepsilon \approx 0.4$. The relative error in minimum fluidisation (X-axis) is larger compared to the relative error in porosity (Y-axis).

Table 1
Richardson-Zaki index equations form literature.

	Reference	Formula	Equation nr.
Classical Richardson-Zaki equation	[13,32]	$n = \begin{cases} Re_t<0.2, & n = 4.65 \\ 0.2 \le Re_t<1, & n = 4.4\, Re_t^{-0.03} \\ 1 \le Re_t<500, & n = 4.4\, Re_t^{-0.1} \\ Re_t \ge 500, & n = 2.4 \end{cases}$	(5)
General expression	[33]	$n = c_1\, Re_t^{c_2}$	(6)
Garside & Al-Dibouni equation	[34,35]	$\frac{n_L - n}{n - n_T} = \alpha\, Re_t^{\beta}$	(7)
Khan & Richardson	[36]	$\frac{n_L - n}{n - n_T} = \alpha\, Ar^{\beta}$	(8)

$< n <$ 4.8, high values are reported by Capes [49], Chong et al. [50] and Johnson et al. [51], often due to the irregularity of investigated grains.

Based on experimental data, some works like [31] on the Richardson-Zaki index n show significant deviation. In other works [12], particle size distributions [10,33,49] affect the linearity of the log v_s versus log ε curves, where particularly at higher flow regimes this leads to deviations in n. Exclusively considering perfectly round monodispersed spheres will show no deviation in n. However, using natural grains, a certain degree of deviation will de facto be observed. By applying irregularly shaped particles, a shape factor [20] could be introduced as a correction for the particle diameter used in the Richardson-Zaki model. Shape factors are often applied in fixed bed processes. In fluidised processes, however, shape factors as a constant correction factor are less accurate due to the re-orientation of irregularly shaped particles that takes place at different porosities. Since the Richardson-Zaki model can solely be used for the fluidised state, pragmatic shape factors are therefore less useful. To be able to cope with irregularity accurately, the Richardson-Zaki model must be extended thoroughly by introducing complex models, even if this might adversely affect the 'elegance' of the simple expression 1. We based our model on spheres, as is commonly done and reported in the literature. Including the irregularity of particles is recommended for future research; at this moment, our measurements lack a detailed quantification of these irregularities.

2.4. The Richardson-Zaki curve

The index n can be determined through the linear relationship between the logarithm of the superficial velocity and the logarithm of the porosity [20,28]. When the plot of log v_s versus log ε for concentrated suspensions is linearly extrapolated to log $\varepsilon = 1$, the intercept is equal to log v_E, where according to Coulson & Richardson v_E is the apparent free falling settling velocity of a particle in an unbounded solution which corresponds closely to the free falling or terminal settling velocity v_t of a single particle. Here, wall effects[2] corrections are introduced.

Chong et al. [50] found the term v_E obtained by linearly extrapolating below $\varepsilon = 0.9$–1 on a log-log plot of v_s versus ε to be measurably lower than the corresponding terminal settling velocity v_t. Dharmarajah [15] stated that Richardson & Zaki failed to observe beyond a porosity of approximately $\varepsilon = 0.9$ where the log v_s versus log ε plots deviate significantly from linearity. Dharmarajah [15] mentioned that the curvature is more pronounced with increasing particle Reynolds numbers and that the characteristics of a liquid fluidised system change drastically when the expanded bed porosity approaches unity. Gibilaro [18] reports that it has been widely verified that a plot of v_s against ε on logarithmical co-ordinates approximates closely to a straight line of bed expansion, regardless of flow regime. However, small deviations from this behaviour have been reported for high void fractions $\varepsilon > 0.95$.

Di Felice [41] described two types of expansion characteristics in which the first region concerns lower porosities and in which a straight line with extrapolation to porosity equal to 1 is below the predicted value of the single particle terminal velocity. In the second region, the slope increases with increasing void fraction, approaching the correct value for v_t. Later, Di Felice & Rotondi [52] reported that values of v_E can also exceed the value of v_t. Analysis of the data sets reported by Girimonte & Vivacqua [53] and Girimonte & Vivacqua [54] indicates that calculated values of v_E are regularly smaller than experimental ones, with an average error of about 25% and a level of inaccuracy that increases as the size of the fluidised particles decreases. Their plotted experimental data clearly deviate increasingly at porosities higher than 0.8.

The intercept velocity or the extrapolated value of the fluid superficial velocity to $\varepsilon = 1$ agreed quite well with the mean terminal settling velocity of a cloud of particles experimentally determined by Đuriš et al. [55]. The experimental data reported by Đuriš et al. [12] at a higher velocity of approximately 10%, however, indicate a deviation of v_E through linear extrapolation of v_s and the terminal settling velocity resulting from the influence of the particle roughness on the behaviour of the bed in high porosity regions during the fluidisation of sand mixtures.

2.5. Richardson-Zaki on the basis of hydraulics

In [20,29,36] a more hydraulics-based approach can be found in which Eq. (1) is rearranged for an explicit equation for the index n at incipient conditions:

$$n = \frac{log\left(\frac{v_{mf}}{v_t}\right)}{log\varepsilon_{mf}} \tag{9}$$

Under extreme conditions, in other words when the minimum fluidisation velocity as well as the terminal settling velocity are known, the index n could be determined. Using the particle Reynolds numbers for terminal settling (Eq. (3)) and the particle Reynolds numbers for minimum fluidisation (Eq. (12)), the index can be written as follows [18]:

$$n = \frac{\log\left(\frac{Re_{\varepsilon,mf}}{Re_t}(1-\varepsilon_{mf})\right)}{\log\varepsilon_{mf}} \tag{10}$$

With:

$$Re_\varepsilon = \frac{\rho_f d_p v_s}{\eta}\frac{1}{1-\varepsilon} \tag{11}$$

Where ϵ becomes ϵ_{mf} and v_s becomes v_{mf} under minimum fluidisation state:

$$Re_{\varepsilon,mf} = \frac{\rho_f d_p v_{mf}}{\eta}\frac{1}{1-\varepsilon_{mf}} \tag{12}$$

3. Richardson-Zaki models and theory related to the fluidised bed pellet-softening process

3.1. Richardson-Zaki water treatment constraints

In pellet-softening reactors, the calcium carbonate pellets range from 1 to 2 mm in size, while for the seeding materials particle size varies between 0.2 mm in case of garnet grains (Fig. 1A) and 0.5 mm when crushed calcite grains are used (Fig. 1C). In full-scale reactors, the superficial velocity is controlled between 60 and 90–120 m/h. In Fig. 3, the operational field is marked green in which the influence of particle size is plotted using the Richardson-Zaki equation.

Fig. 4 shows the effect of the magnitude of n on porosity in relation to the superficial velocity for a given particle size. The terminal settling velocity increases when particles grow in size: this can be determined with the Richardson-Zaki equation with an assumed porosity $\varepsilon \to 1$. In case the terminal settling velocity is known, the index n can be calculated for several models. For a given minimum fluidisation porosity, the subsequently estimated minimum fluidisation velocity leads to significant deviations.

3.2. Hydraulics-basedRichardson-Zaki index

In the literature [21,56,57], several equations have been proposed for equations for n. These works, however, have not used the latest hydraulic models. To develop an accurate Richardson-Zaki index

[2] See Supplementary Materials for Richardson-Zaki index equations and wall effects corrections.

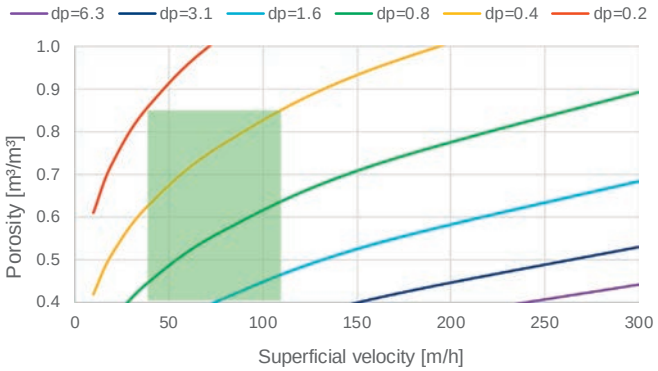

Fig. 3. The effect of particle size (values in mm at the top) and superficial velocity (X-axis) on porosity predicted by Richardson-Zaki. The green area marks the operation range of drinking water pellet-softening fluidisation processes regarding seeded calcium carbonate crystallisation. (For interpretation of the references to colour in this figure legend, the reader is referred to the web version of this article.)

expression, Eq. (9) is used as a starting point. Besides the minimum fluidisation porosity ε_{mf}, also the terminal settling velocity and the minimum fluidisation velocity are required.

In the literature [58–63], a comprehensive collection of widely used models is available to estimate the drag and terminal settling velocity of particles. A well-know and accepted model is the Brown-Lawler [64] Eq. (13) which is an improved model of the well-known equation proposed by Schiller & Naumann [65]. This is discussed in Kramer et al. [63].

$$C_D = \frac{24}{Re_t}\left(1 + 0.15 Re_t^{0.681}\right) + \frac{0.407}{1 + \frac{8710}{Re_t}} \quad (Re_t < 200,000) \tag{13}$$

Since terminal settling velocity is an important variable in the Richardson-Zaki Eq. (1), the effect of particle properties may considerably affect the numerical outcome of the index n and the estimated minimum fluidisation velocity.

The Richardson-Zaki model does not provide any information about the porosity at minimum fluidisation. This is also the case for hydraulics-based models such as Kozeny, Carman and Ergun. Nevertheless, using the steady state force balance for suspensions at incipient fluidisation state, makes it possible to introduce the porosity at minimum fluidisation.

A frequently used equation to calculate the pressure drop of a fluid flowing through a packed bed of solids for laminar flow is the Kozeny equation [66]:

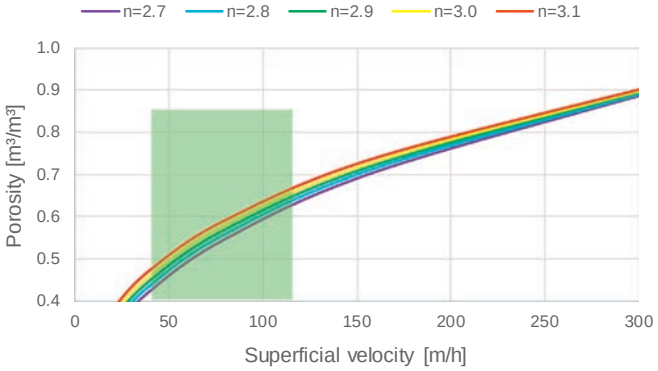

Fig. 4. The influence of the Richardson-Zaki index for a particular grain, e.g. $d_p = 0.8$ [mm]. The green area marks the operation range of drinking water pellet-softening fluidisation processes. The effect of e.g. 10% deviation in v_t or v_E on porosity in drinking water softening process is relative small 12% however larger for minimum fluidisation velocity 47%. (For interpretation of the references to colour in this figure legend, the reader is referred to the web version of this article.)

$$\frac{\Delta P}{\Delta L} = 180 \frac{v_s \eta}{{d_p}^2} \frac{(1-\varepsilon)^2}{\varepsilon^3} \tag{14}$$

The corresponding Kozeny friction factor C_D states:

$$C_D = \frac{180}{Re_\varepsilon} \quad (Re_\varepsilon < 2) \tag{15}$$

where Re_ε is defined in Eq. (11). Carman [67] as well as [68,69] proposed an extension,[3] resulting in a second term for the transitional flow regime and valid for a higher particle Reynolds number (Eq. (11)).

$$C_D = \frac{180}{Re_\varepsilon} + \frac{2.87}{{Re_\varepsilon}^{0.1}} \quad (Re_\varepsilon < 600) \tag{16}$$

For higher flow regimes, Ergun [70] is frequently used to calculate the friction factor C_D according to Eq. (17):

$$C_D = \frac{150}{Re_\varepsilon} + 1.75 \tag{17}$$

Accordingly, the Richardson-Zaki index n can be determined by combining the rearranged Eq. (9) with the Carman-Kozeny Equation (16) and the Brown-Lawler Equation (13). For both equations, numerical solver methods are required to solve the porosity for applied boundary conditions: ($Re_t < 200,000$) and ($Re_\varepsilon < 600$). Today, using this model should not present any obstacles. This model is abbreviated to *RZ-hydr1 (CK + BL)*.

3.3. Simplified analytical expressions

Although numerical solvers can be used for the porosity, it is desirable to have available analytical expressions that do not need an iterative numerical approach. Accordingly, several analytic models are given. It is possible to derive an explicit model using an simplified drag equation based on Lewis et al. [71], Clark [72] and Kunii & Levenspiel [73]:

$$C_D = \frac{10}{\sqrt{Re_t}} \quad (0.4 < Re_t < 500) \tag{18}$$

A more general form [21] of Eq. (18) is:

$$C_D = \alpha \, {Re_t}^{\beta} \tag{19}$$

in which the Lewis coefficients are $\alpha = 10$ and $\beta = -0.5$. For other frequently used equations, e.g. Oka & Anthony [21], the coefficients are $\alpha = 18.5$ and $\beta = -0.6$. The value $\beta = -0.5$ results in a linear relationship between drag and the terminal settling velocity [74], which confirms that calcite pellets are in the middle of the transitional flow regime.

[3] The information regarding Kozeny, Carman and Ergun equations are given in the Supplementary Materials.

3.3.1. Kozeny-Lewis hydraulic analytic model

Using the particle Reynolds terminal Eq. (3) and the Kozeny drag Eq. (14), the Richardson-Zaki index equation becomes the following[4]:

$$n = \frac{log\left(\frac{3}{4}\alpha\frac{{Re_t}^{\beta+1}}{180}\frac{{\varepsilon_{mf}}^3}{1-\varepsilon_{mf}}\right)}{log\varepsilon_{mf}} \quad (5 < Re_t < 500) \tag{20}$$

Eq. (20) is bounded between thresholds for the particle Reynolds numbers (Eq. (12)) at minimum fluidisation conditions and for the terminal Reynolds number at intermediate range.

In the literature, expressions are also given for the Archimedes number (Eq. (4)), as a result of which Eq. (20) becomes the following:

$$n = \frac{log\left(\frac{Ar^{\frac{\beta+1}{\beta+2}}}{180}\frac{{\varepsilon_{mf}}^3}{1-\varepsilon_{mf}}\left(\frac{3}{4}\alpha\right)^{\frac{1}{\beta+2}}\right)}{log\varepsilon_{mf}} \quad (10<Ar<80,000) \tag{21}$$

This model is abbreviated to: *RZ-hydr2 (KZ + LW)*.

3.3.2. Kozeny-Lewis hydraulic extended analytic model

Gibilaro [18] presented the Kozeny Eq. (14) Combine the sentences with:

$$\frac{\Delta P}{\Delta L} = C_D\frac{\rho_f {v_{mf}}^2}{d_p}\frac{1-\varepsilon_{mf}}{{\varepsilon_{mf}}^3} \tag{22}$$

Van Dijk & Wilms [4] adjusted the Kozeny equation through the adjustment of the friction factor and used different coefficients $\kappa = 130$ and $\lambda = -0.8$. A more general form of C_D is:

$$C_D = \kappa\, {Re_\varepsilon}^{\lambda} \tag{23}$$

Now, the Richardson-Zaki index equation becomes as follows:

$$n = \frac{log\left(Re_t^{\frac{\beta-\lambda}{\lambda+2}}\left(\frac{{\varepsilon_{mf}}^3\left(1-\varepsilon_{mf}\right)^{\lambda}}{\kappa}\right)^{\frac{1}{\lambda+2}}\left(\frac{3}{4}\alpha\right)^{\frac{1}{\lambda+2}}\right)}{log\varepsilon_{mf}} \tag{24}$$

$$n = \frac{log\left(Ar^{\frac{\beta-\lambda}{(\beta+2)(\lambda+2)}}\left(\frac{{\varepsilon_{mf}}^3\left(1-\varepsilon_{mf}\right)^{\lambda}}{\kappa}\right)^{\frac{1}{\lambda+2}}\left(\frac{3}{4}\alpha\right)^{\frac{1}{\beta+2}}\right)}{log\varepsilon_{mf}} \tag{25}$$

Eq. (20) is retrieved for the Kozeny coefficients $\kappa = 180$ and $\lambda = -1$.

3.3.3. Ergun-Lewis hydraulic analytic model

The next model is abbreviated to *RZ-hydr3 (EG + LW)* and is based on the Ergun-Archimedes Eq. (26) and the Lewis Eq. (18).

$$Ar = A\, Re_{\varepsilon,mf} + B\, {Re_{\varepsilon,mf}}^2\frac{1-{\varepsilon_{mf}}^2}{{\varepsilon_{mf}}^3} \tag{26}$$

where A = 150, B = 1.75 = 7/3.

[4] The derivations of equation Kozeny-Lewis n Eq. (20), (21), van Dijk variants 24, 25, Ergun-Lewis Eq. (27) and floating parameters 29, 28, 31 and 30 can be found in the Supplementary materials.

The following analytic Richardson-Zaki index equation can be derived:

$$n = \frac{log\left(\frac{\sqrt{\left(\frac{1}{2}\frac{A}{B}\left(1-\varepsilon_{mf}\right)\right)^2 + \frac{{\varepsilon_{mf}}^3}{B}Ar} - \frac{1}{2}\frac{A}{B}\left(1-\varepsilon_{mf}\right)}{\left(\frac{4}{3}\frac{Ar}{\alpha}\right)^{\frac{1}{\beta+2}}}\right)}{log\varepsilon_{mf}} \quad (10<Ar<300,000) \tag{27}$$

When the second term of Eqs. (17) or (26) is ignored, Eq. (20) is retrieved; however, this is done with the Ergun coefficient 150 instead of the Kozeny value 180.

3.3.4. Floating parameters

It is also possible to find an implicit analytical solution for Eq. (20) with the same numerical output of the Brown-Lawler and Carman-Kozeny models. This can be achieved by using the principle of simple drag Eqs. (19) and (23) with so-called floating coefficients α, β as a function of the particle Reynold terminal number and κ, λ as a function of the particle Reynolds minimal fluidisation number. The result is as follows:

$$\beta = \frac{\frac{c_1\left(c_2\left(c_3-1\right){Re_t}^{c_3}-1\right)}{{Re_t}^2} + \frac{c_4 c_5}{\left(Re_t + c_5\right)^2}Re_t}{\frac{c_1}{Re_t}\left(1 + c_2{Re_t}^{c_3}\right) + \frac{c_4}{1+\frac{c_5}{Re_t}}} \tag{28}$$

$$\alpha = \frac{\frac{c_1}{Re_t}\left(1 + c_2{Re_t}^{c_3}\right) + \frac{c_4}{1+\frac{c_5}{Re_t}}}{{Re_t}^{\beta}} \tag{29}$$

$$\lambda = \frac{-\frac{c_1}{{Re_\varepsilon}^2} - c_2 c_3 {Re_\varepsilon}^{-c_3-1}}{\frac{c_1}{Re_\varepsilon} + \frac{c_2}{{Re_\varepsilon}^{c_3}}}Re_\varepsilon \tag{30}$$

$$\kappa = \frac{\frac{c_1}{Re_\varepsilon} + \frac{c_2}{{Re_\varepsilon}^{c_3}}}{{Re_\varepsilon}^{\lambda}} \tag{31}$$

Finally, the coefficients in Eqs. (7) and (8) can be numerically fitted with the Brown-Lawler + Carman-Kozeny index functions (Eqs. (13) and (16)). These models are abbreviated to *RZ-hydr-Ret* and *RZ-hydr-Ar*.

4. Materials and methods

4.1. Experimental setup

Expansion experiments for several materials were carried out in Waternet's Weesperkarspel drinking water pilot plant located in Amsterdam, the Netherlands. In the experiments, the produced drinking water was used. The setup (Fig. 5) consisted of a 4-meter transparent PVC pipe with an inner diameter of 57 mm. Water temperature was regulated with a boiler, a cooler and a thermostat by recirculating water through a buffer vessel connected to a water reservoir. An overflow at the top of the reactor returned water to the buffer vessel. From the buffer vessel, water was pumped through the reservoir connected to the thermostat which was set to a programmed water temperature. During the terminal settling experiments, the water pump was turned off.

4.2. Particle selection

In this study, we examined predominantly natural particles which are frequently applied in drinking water treatment processes, in

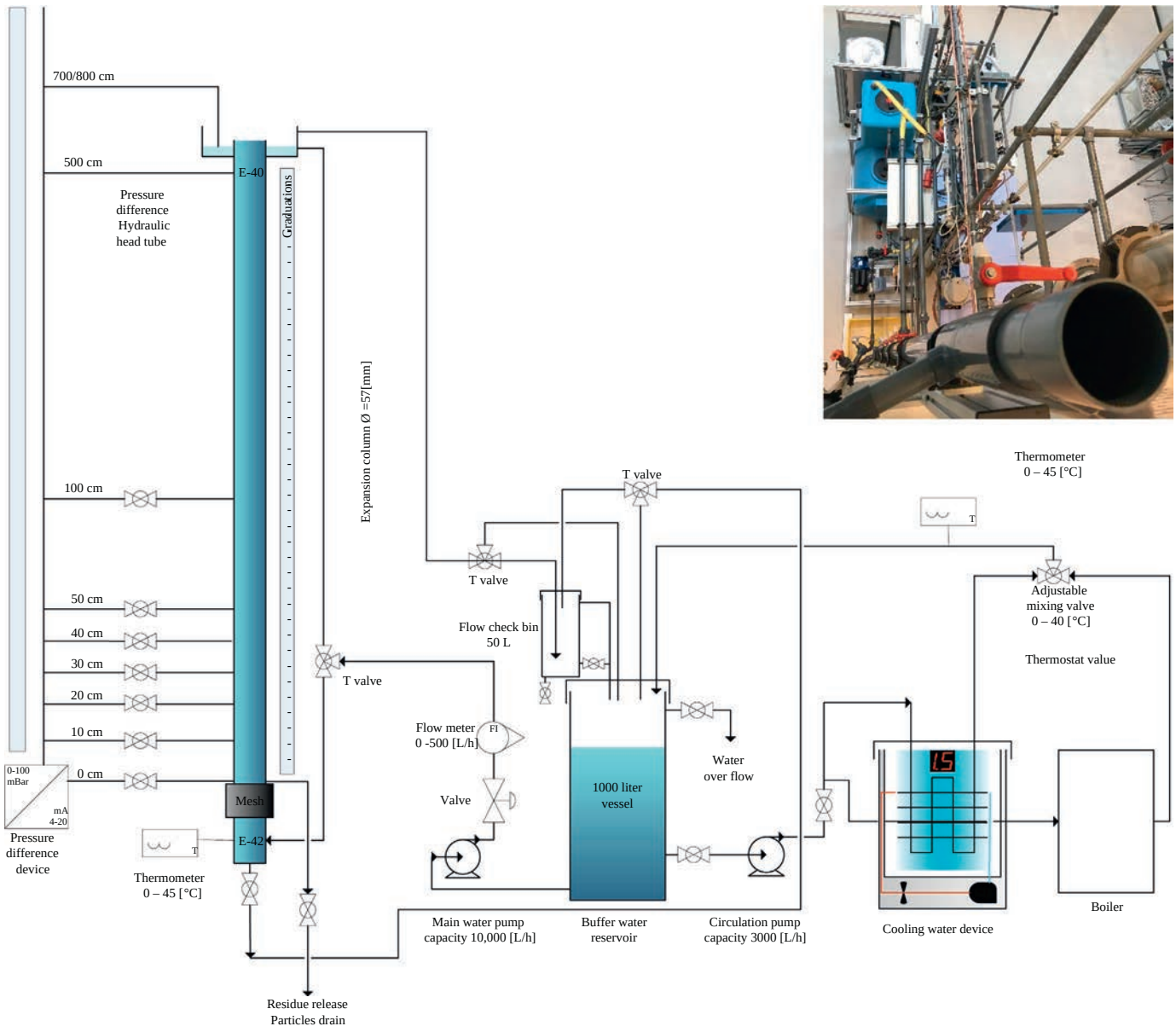

Fig. 5. Experimental setup.

particular in the softening process. Investigations started with garnet grains, the most frequently utilised seeding material in the Netherlands, calcite pellets, which is seeding material with a substantial layer of crystallised $CaCO_3$ coming from the softening process and also re-used crushed calcite, processed in the Netherlands. Garnet grains and calcite pellets were dried at room temperature; crushed calcite grains were dried in an oven at 150–200 °C for hygiene purposes.

In this research, we selected garnet grains as well as calcite pellets in which the core consists of pure calcite as well as crushed calcite grains given in Table 2.

Particles were initially sieved and separated in order to acquire more uniformly dispersed samples with a defined sieve diameter in which the hydraulic equivalent particle diameter could be calculated using Eq. (32). Available sieve sizes are usually regulated by standards such as ISO 3310-1 (NEN-norm [75]) and ASTM E11:01 (US). The distance between succeeding sieve openings varies between 2, √2 and 1.20 and 1.12. In this research, the ratios between two succeeding sieve openings were 1.12 and 1.20.

4.3. Particle and fluid characterisation

4.3.1. Average particle diameter

The effective or average hydraulic equivalent particle diameter d_p was based on the applied sieve method in which particles were divided over the slides of sieves and calculated according to the appropriate geometric mean for two sieves:

$$d_p = \sqrt{d_{s,1} d_{s,2}} \tag{32}$$

4.3.2. Particle density

The density of the grain material was measured with a 50 mL pycnometer [76]. In advance, particle density was validated using the experimental setup where the pressure drop in a homogenous fluidisation state is independent of the prevalent superficial fluid

Table 2
Particle materials.

Grain material	Mesh bottom sieve [μm]	Mesh top sieve [μm]	Average grain size [mm]	Frequency [#]
Garnet grains (mesh 80)	212	250	0.23	5
Garnet grains (mesh 30/60)	250	300	0.27	8
Crushed calcite	400	500	0.45	4
”	400	600	0.49	4
“	500	600	0.55	4
“	500	630	0.56	8
Calcite pellets	425	500	0.46	4
“	500	600	0.55	4
“	600	710	0.65	4
“	710	800	0.75	4
“	800	900	0.85	4
“	900	1120	1.00	11
“	1120	1400	1.25	4
“	1400	1700	1.54	4
“	1700	2000	1.84	4

velocity. The particle density can be determined accurately using Eq. (33).

$$\Delta P = \frac{mg}{\frac{\pi}{4}D^2}\,\frac{\left(\rho_p-\rho_f\right)}{\rho_p} \tag{33}$$

Due to crystallisation of $CaCO_3$ at the particle surface, particle size increases. Since the density of the seeding material, for instance garnet grains, is different from the density of calcium carbonate, the average density changes during the softening process. Eq. (34) was used to estimate average particle density for garnet pellets based on the assumption that round particles contain an equally distributed layer of pure chalk with a density of 2711 kg/m^3, as postulated by Anthony [77].

$$d_p{}^3\rho_p = d_g{}^3\rho_g + \left(d_p{}^3-d_g{}^3\right)\rho_c \tag{34}$$

4.3.3. Physical properties of water

The density of ordinary water as a function of temperature was retrieved from Haynes [78], Perry [79] and Albright [80]. The dynamic viscosity is given by the Vogel-Fulcher-Tammann equations [81,82]. In these equations, the influence of the combined content of all inorganic and organic substances (Total Dissolved Solids, TDS = 400 mg/L) is small, (0.03% for the density and 0.07% for the dynamics viscosity [83]), and has not been taken into account as appropriate for applied drinking water.

4.4. Terminal settling velocity experiments

In the current study, the settling behaviour of single particles was determined through adjusting the water temperature for various materials and for different grain sizes. The temperature was carefully controlled by flowing water through the column of the exact temperature before each experiment and by regularly repeating this process throughout the experiment. Individual particles were dropped at the top of the column. After steady state velocity had been reached, the required time to elapse a defined distance ($L = 2$ m) was measured visually. All fractions in Table 2 were tested for temperatures between 3 and 36 °C. A powerful flashlight at the top of the column supported the visual determination [63] of the free falling particles.

4.5. Fluidisation expansion experiments

4.5.1. Standard operating procedure

Fluidisation behaviour was examined for a set of different grains varying in size, shape and composition. The test column was filled with approximately 0.3–3.0 kg of uniform particles. To prepare the experiments, the particles were initially gently fluidised until the suspension was stratified on size, shape and particle density. The flow was stopped, and after the particle bed had settled into a fixed state, the fixed bed height was measured. Then, the flow velocity was slowly increased. For each flow velocity, bed height and pressure difference were recorded individually. The pressure difference was measured with a device as well as hydrostatically. The pressure difference was corrected for both the hydrodynamic influence $½\rho v^2$, which had a minor effect, and for missing mass ($L/(L$-0.03), since the lowest pressure sensor was assembled at 3 cm above the bottom of the column.

The water flow was gradually increased until the particles were in an incipient state and started to fluidise. The minimum fluidisation bed height was not only measured visually but also determined based on the intersection of linearly increasing pressure difference in the fixed bed state and the maximum pressure difference in the homogeneous fluidisation condition. The water temperature was kept constant during the experiments and was measured at the overflow of the column and directly in the column. Expansion experiments were conducted for garnet grains and calcite pellets for at least four different water temperatures between 3 and 36 °C. For each individual experiment, the temperature was recorded at least four times. For crushed calcite, the temperature was recorded for every single measurement. Since the experimental setup had been improved technically, pressure differences were absent in some of the experiments.

In total, 76 fluidisation expansion experiments were carried out. Regarding calcite pellets and garnet grains, the superficial velocity was increased until approximately 180 [m/h] and for crushed calcite until approximately 260 [m/h].

The data derived from the expansion experiments were used to calculate pressure difference, bed porosity and average particle size. The calculated pressure difference was compared with the measured sensor and hydrostatic values. The calculated porosity was compared with the porosity derived directly from the experimental data. The average particle diameter was derived from the applied sieve fractions.

For every experiment, an expansion curve was plotted with bed porosity, pressure difference and transitions from fixed to fluidised state.

4.5.2. Bed porosity and expansion

Because the initial amount of grains is known, the fixed and fluid bed porosity and expansion can be calculated using Eqs. (35) and (36):

$$\varepsilon_0 = 1-\frac{m}{\frac{\pi}{4}D^2L_0\rho_p} \tag{35}$$

$$E = \frac{L}{L_0} = \frac{1-\varepsilon_0}{1-\varepsilon} \tag{36}$$

4.5.3. Pressure difference

In the steady state of homogeneous fluidisation of particulate solids, the pressure drop equals the weight of the bed material, reduced by the buoyancy forces, per unit of bed surface. The experimental data was validated using Eq. (37):

$$\frac{\Delta P}{\Delta L} = \left(\rho_p-\rho_f\right)g\left(1-\varepsilon_{mf}\right) \tag{37}$$

Table 3
Grain materials.

Grain material	Type	Number of individual experiments [#]	Grain size [mm]	Particle density measured [kg/m^3]	Particle density validated (Eq. (33)) [kg/m^3]	Fixed bed porosity (Eq. (35)) [m^3/m^3]	Minimum fluidisation porosity [m^3/m^3]
Garnet grains	Seeding material	13	0.21–0.30	4175 ± 25	4040 ± 125	0.44 ± 0.02	0.46 ± 0.03
Crushed calcite	Seeding material	20	0.40–0.63	2575 ± 5	2570 ± 50	0.49 ± 0.01	0.51 ± 0.01
Calcite pellets	$CaCO_3$ grains	43	0.43–2.00	2625 ± 35	2703 ± 50	0.38 ± 0.01	0.40 ± 0.01

4.5.4. Statistical methods

To compare the experimental data with the prediction models, the average relative error [64,84] is determined as:

$$ARE = \frac{1}{n}\sum_{i=1}^{n}\left(\frac{|y_{calc,i} - y_{exp,i}|}{y_{exp,i}}\right) \tag{38}$$

In Section 5, we will compare the various equations presented in Section 3 with data obtained from our experimental setup in Section 4. We will evaluate the performance and accuracy of the various equations, and we will formulate our advice on the best approach for practical applications.

5. Results and discussion

5.1. Obtained particle properties

The experimentally measured particle density of examined grains is given in Table 3. An average relative error of 2% was found in the particle density, caused by both the laboratory experiments and natural variations of the particle properties. The average particle density was derived (Eq. (33)) from the fluidised bed setup based on the pressure drop measurement. The average relative error here was 3%. The measured fixed bed porosity for calcite pellets (Table 3) agrees with an expected value of 0.4 for round spheres. Garnet grains, which were mined and had a more irregular shape, show a higher fixed bed porosity. The fixed bed porosity of crushed calcite seeding material, with a much more irregular shape due to crushing, is significantly higher, which also agrees with findings reported by Wen & Yu [85], Yang [20] and Đuriš [12].

5.2. Expansion experiments

The acquired experimental data set consisted of a matrix with varied temperature, grain size and flow, as was required for a comparison of the theoretical fluidisation models.

In total, 76 fluidisation experiments[5] were carried out for calcite pellets, garnet and crushed calcite grains. Fig. 6 shows, as an example, a typical expansion curve in which the porosity and pressure difference was measured for increasing superficial velocity.

In their original article, Richardson & Zaki plotted superficial velocity in the opposite way on logarithmic scales. Both in Fig. 6 and Fig. 7, the incipient fluidisation points are clearly visible. The Richardson-Zaki line intercepts at $\varepsilon = 1$ the apparent free-falling settling velocity v_E of a particle at infinite dilution. Note that in this example, v_E is 4% lower than the estimated terminal settling velocity calculated with Eq. (13).

For the 76 fluidisation experiments, the extrapolated fluid velocity v_E was determined: this is displayed in Fig. 8, showing that in particular for higher velocities, the deviations increase. For the calcite pellets, the deviations may be caused by inaccurate extrapolation to $\varepsilon \to 1$ since the maximum obtained porosity was 0.6 for large pellets ($d_z > 1.4$ mm) during the expansion experiments. The value of v_E for crushed calcite is lower than v_t, which is due to the highly irregularly shaped particles - something that becomes more apparent for higher fluid velocities, which in turn leads to more unsteady drag behaviour.

5.3. Minimum fluidisation velocity prediction

The porosity at minimum fluidisation is a crucial parameter and in fact more important than the terminal settling point, since the process state in pellet-softening reactors and apparent porosity are closer to the state of minimum fluidisation. With Eqs. (35) and (36), both the fixed and incipient bed porosity were calculated for 76 experiments.

Three groups of models were compared with respect to their ability to predict the minimum fluidisation velocity accurately. Table 4 shows the results for Richardson-Zaki-based models, followed by frequently used hydraulic models as reported in the literature and thirdly by Richardson-Zaki hydraulics-based models. The prediction accuracy of the first group is generally low, compared to the second group. This result can also be observed in Fig. 9. A global explanation is that Richardson-Zaki starts with the terminal settling point and has to predict v_{mf} using a slope n over a large porosity 'distance' ($\Delta\varepsilon \approx 0.6$) with the possibility of overestimation. Because the models of the second groups are based

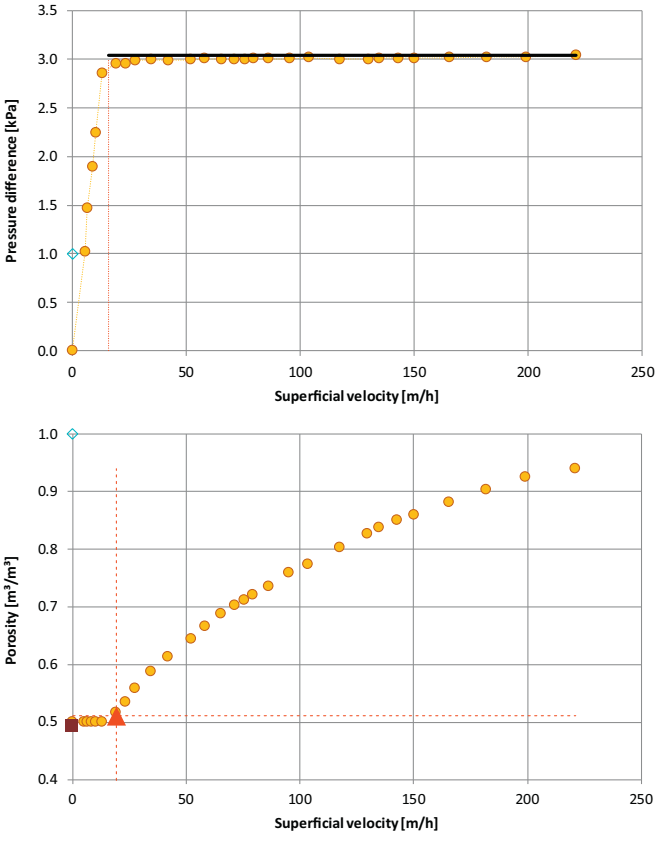

Fig. 6. A typical expansion experiment concerning crushed calcite grains $0.5 < d_p < 0.6$ mm, T = 25 °C with measured pressure difference (Eq. (37)) and porosity (Eq. (35)). The vertical red line indicates the minimum fluidization velocity. L-S Fluidisation experiment nr.: 63.

[5] All experimental data of expansion experiments can be found in the Supplementary Materials.

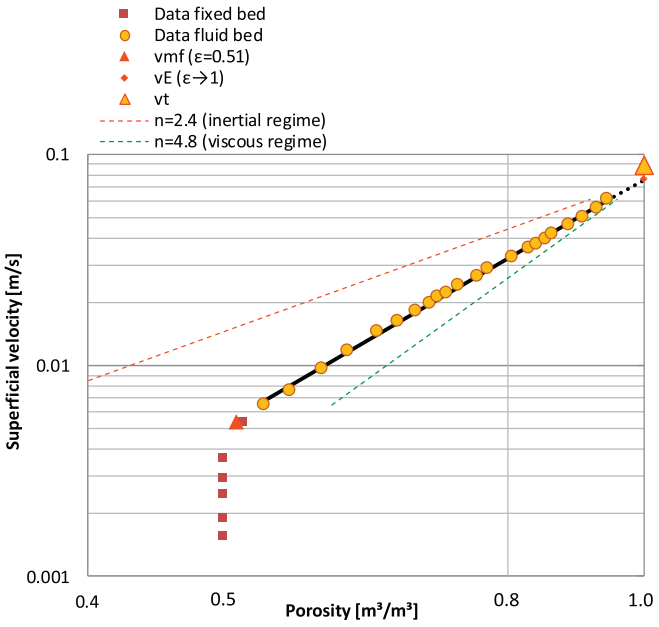

Fig. 7. Richardson-Zaki representation. L-S Fluidisation experiment nr.: 63.

on the principle of fixed state, it seems evident that their prediction is much more accurate. Based on the experiments, the Carman-Kozeny model was found to have the lowest error: it can therefore be considered the best model to predict the minimum fluidisation point. The models in the third group are based on both Richardson-Zaki and the classical hydraulic models and provide a lower error compared the first group. The hydraulics-based Richardson-Zaki numerical model *RZ-hydr1 (BL + CK)* is slightly less accurate than the Carman-Kozeny model.

5.4. Porosity prediction

Porosity prediction accuracy was determined for three different ranges. This was first done for a wide operation range regarding pellet-softening: 60–90 m/h, for superficial velocities up to 180 m/h and for a wide examined fluid flow range applied in the expansion experiments. The average relative errors (Eq. (38)) were calculated for 76 experiments: these are listed in Fig. 10. The original Richardson-Zaki model has an error of 8% for a wide range of fluid velocity. This error increases to 17% for grains applied in the drinking water pellet-softening process. The Richardson-Zaki model built on a hydraulic basis, as derived in this work, provides much lower errors of approximately 3%. A particular point of interest concerns taking into account the validity of the working area.

Table 4
Minimum fluidisation velocity prediction.

Model	Reference	Equations	Average relative error [%]
Group 1: Richardson-Zaki models from literature			
Richardson-Zaki	[13]	1, 3, 5	100.4%
Rowe	[35]	1, 4, 7	106.3%
Wallis	[86]	1, 3, 7	63.6%
Garside-AlDibouni	[34]	1, 3, 7	52.9%
Khan-Richardson	[36]	1, 4, 8	51.9%
Van Schagen	[87]	1, 3, 5	87.6%
Group 2: Hydraulic models			
Kozeny	[66]	37, 14	26.2%
Carman-Kozeny	[67]	37, 16	12.4%
Ergun	[70]	37, 17	29.6%
Group 3: Richardson-Zaki hydraulics-based models			
RZ-hydr1 (BL + CK)		1, 16, 13	13.1%
RZ-hydr2 (KZ + LW)		1, 20	15.7%
RZ-hydr3 (EG + LW)		1, 27	20.6%
RZ-hydr-Ret		1, 3, 39	16.4%
RZ-hydr-Ar		1, 4, 40	16.8%

5.5. Richardson-Zaki index

The models proposed by Richardson-Zaki, Rowe, Wallis, Garside-*Al* Dibouni and Khan-Richardson use the index n to predict porosity (Eq. (1)). In Fig. 11, the determined indices n for 76 experiments are plotted (dots) as well as the curves for given models. All examined grains applied in the softening process have a higher value compared to the expected Richardson-Zaki values (red curve) and coincide quite well with the Richardson-Zaki hydraulics-based models. This has been confirmed and reported in earlier publications by Siwiec [33] and is due to the irregularity of the grains which will re-orientate during

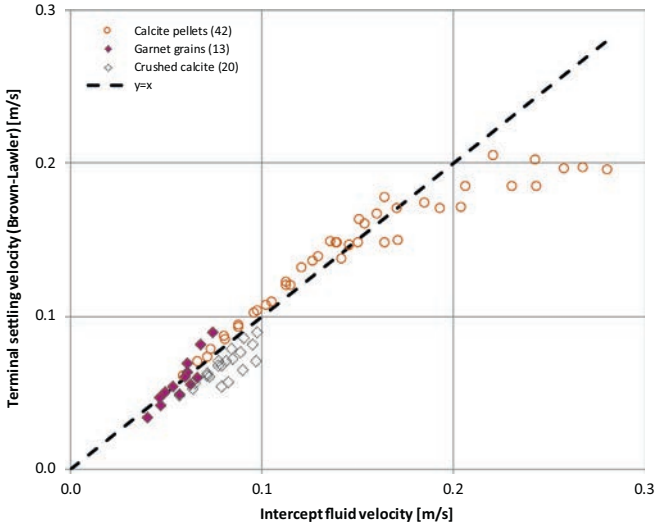

Fig. 8. Terminal settling velocity v_t calculated with the Brown-Lawler Eq. (13) against the Richardson-Zaki intercept velocity v_E. (For interpretation of the references to colour in this figure legend, the reader is referred to the web version of this article.)

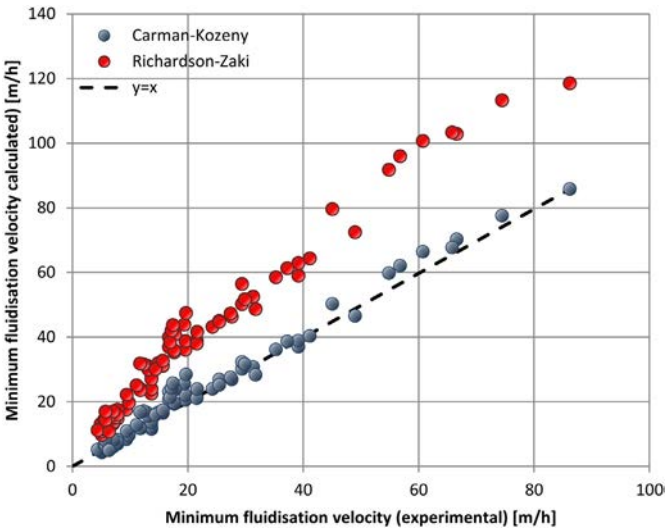

Fig. 9. The experimentally determined minimum fluidisation velocity versus the calculated minimum fluidisation velocity using Richardson-Zaki (Eq. (1)) and Carman-Kozeny (Eq. (16)). Richardson-Zaki overestimates the minimum fluidisation velocity.

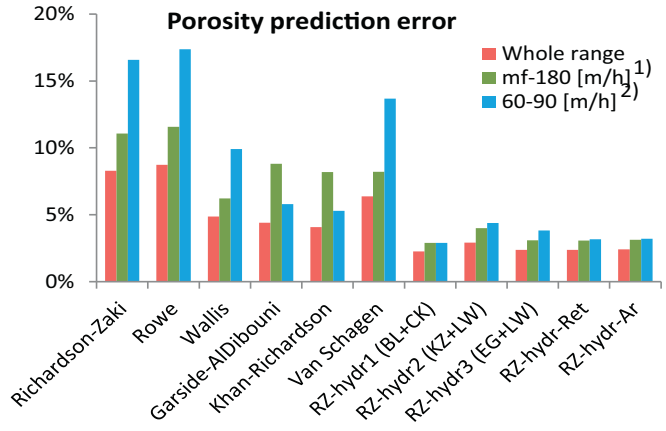

Fig. 10. Relative errors of predicted porosity according to different models from literature and from this work. 1) Starting with the lowest minimum fluidisation velocity. 2) Waternet operational area in softening reactors.

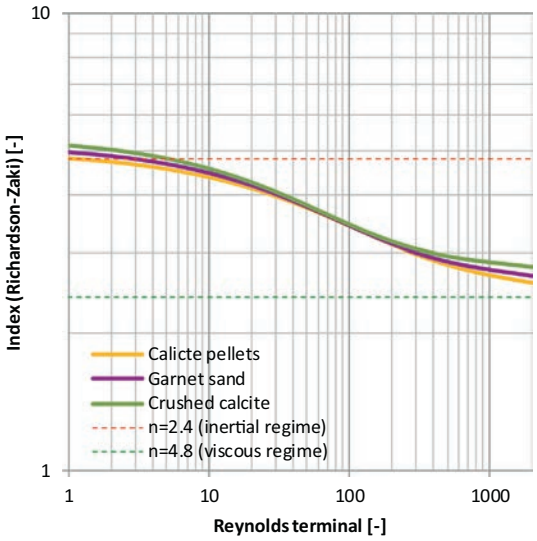

Fig. 12. The influence of specific density and porosity at minimum fluidisation of garnet grains, crushed calcite grains and calcite pellets. See Table 3 for physical properties of particles.

fluidisation, causing the exerting drag to increase and behave like virtually smaller grains with a corresponding higher n value.

Fig. 12 shows the influence on n of having different particles with different hydraulic physical properties, such as incipient porosity ε_{mf} and particle density ρ_p. Despite the fact that at Reynolds terminal ($Re_t \approx 100$) all three curves coincide, the index value increases up to 2% for garnet grains and 7% for calcite grain, both at lower and higher Reynolds terminal values.

In summary, we find that the hydraulics-based Richardson-Zaki model *RZ-hydr1 (BL + CK)* enables us to predict the porosity with a low error, but unfortunately numerical iteration remains necessary. From a pragmatic point of view, it is desirable to be able to predict the porosity with an explicit analytical equation such as the Eqs. 7 and 8. Furthermore, the elegance of Richardson-Zaki is the simplicity of the particular model itself. To allow for fast evaluations, we have numerically fitted the coefficients, based on Brown-Lawler + Carman-Kozeny (Eqs. (13) and (16)): they are presented in Table 5.

This leads to simplified equations:

$$\frac{4.8-n}{n-2.4} = 0.043\, Re_t^{0.75} \tag{39}$$

$$\frac{4.8-n}{n-2.4} = 0.015\, Ar^{0.5} \tag{40}$$

6. Conclusions

The well-known Richardson-Zaki model is frequently cited and successfully applied in varied industries. The reason is its simple mathematic appearance. Its starting point is the falling velocity of a

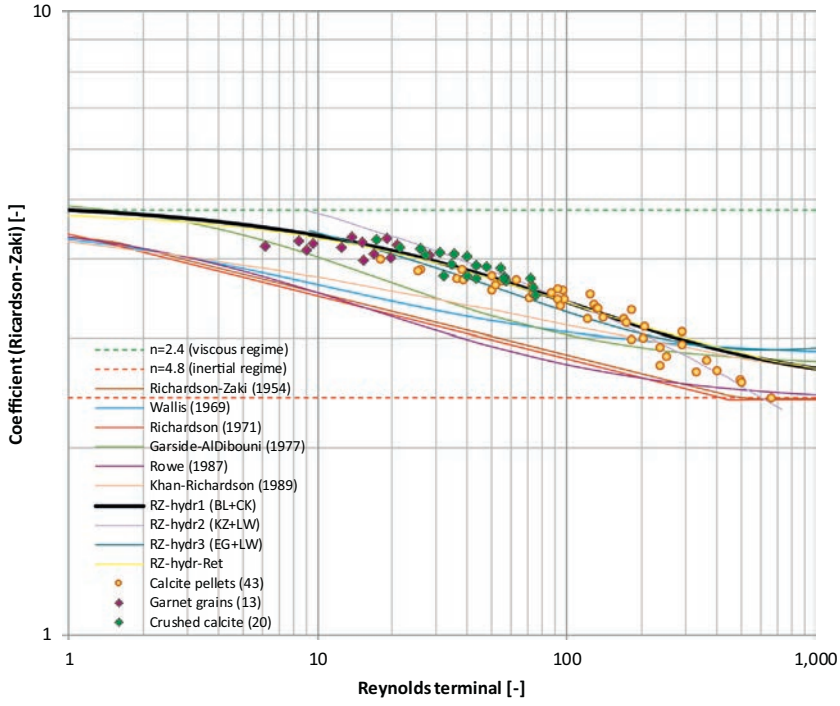

Fig. 11. The experimentally determined Richardson-Zaki index for investigated grains.

Table 5
Coefficients in Eqs. (7) and (8).

Model	Reference	n_L	n_T	$\alpha(Re_t)$	$\beta(Re_t)$	$\alpha(Ar)$	$\beta(Ar)$
Theoretical	[29]	4.8	2.4				
Richardson & Zaki	[13]	4.65	2.4				
Wallis	[86]	4.7	2.79	0.253	0.687		
Garside & *Al*-Dibouni	[34]	5.09	2.73	0.104	0.877		
Garside & *Al*-Dibouni (simplified)	[34]	5.1	2.7	0.1	0.9		
Dharmarajah (forced through ε_{mf})	[15]	5.09	2.73	0.194	0.877		
Rowe	[35]	4.7	2.35	0.175	0.75		
Khan & Richardson	[36]	2.084	4.94	3.24	−0.37		
Khan & Richardson	[36]	4.8	2.4			0.043	0.57
RZ-hydr-Ret	This study	4.8	2.4	0.043	0.75		
RZ-hydr-Ar	This study	4.8	2.4			0.015	0.5

suspension relative to a fixed horizontal plane that equals the upward velocity of the liquid, based on the empty tube, required to maintain a suspension at the same concentration. Thanks to this simple method, the expansion of a liquid-solid fluidised bed can be predicted. However, the prediction of porosity in drinking water treatment processes in the proximity of minimum fluidisation on the basis of the traditional index equations overestimates the measured values of minimum fluidisation. Using an extra hydraulic point with an actual physical meaning makes the porosity prediction a much more accurate one.

Based on the Brown-Lawler equation combined with the Carman-Kozeny equation, porosity can be predicted with an error of approximately 3% for particles applied in pellet-softening processes for drinking water production purposes. When the index n is used to estimate porosity, the influence of n for lower superficial velocities is much higher compared to conditions in the proximity of terminal settling conditions or higher porosities.

The determined index n values in this research show a higher value compared to those expected on the basis of the classic Richardson-Zaki model, something which is due to the irregularity of the considered drinking water grains. The Richardson-Zaki model that is constructed on a hydraulic basis is an improvement on the classical Richardson-Zaki model: the average relative error for porosity decreases from 15% to 3% in the operational working area of liquid-solid pellet-softening within a porosity range of $0.5 < \varepsilon < 0.8$. With respect to minimum fluidisation velocity, the average relative error decreases from 100% to 12%.

Finally, with simplified analytical equations it is possible to make a straightforward estimation of the index *n*.

Nomenclature

A, B, C	Coefficients [−]
Ar	Archimedes number [−]
C_i	Coefficients [−]
C_D	Fluid dynamic drag coefficient [−]
D	Inner column or cylinder vessel diameter [m]
d	Sieve mesh width [m]
d_p	Effective or average or particle equivalent diameter [m]
d_g	Average seeding material diameter [m]
$d_{s,i}$	Sieve mesh diameter [m]
Error	1.96 times standard deviation
E	Bed expansion [%]
f	Correction factor [−]
g	Local gravitational field of earth equivalent to the free-fall acceleration [m/s^2]
k	Wall effects correction multiplier [−]
ΔL	Relative total fluid bed height [m]
L	Fluid bed height [m]
L_0	Fixed bed height [m]
m	Mass [kg]
N	Total number of particles / total number of experiments [#]
n	Richardson-Zaki coefficient, expansion index [−]
n_L	Constant asymptotic value of the Richardson-Zaki index n at low Reynolds terminal [−]
n_T	Constant asymptotic value of the Richardson-Zaki index n at high Reynolds terminal [−]
ΔP	Pressure drop head loss [kPa]
ΔP_x	Pressure drop head loss over column length x [kPa]
ΔP_{max}	Total maximum pressure drop over the bed [kPa]
Q_w	Water flow [m^3/h]
Re_{mf}	Reynolds particle for incipient fluidisation conditions [−]
Re_p	Reynolds particle not (corrected for the porosity) [−]
Re_t	Reynolds particle for terminal velocity conditions [−]
Re_ε	Reynolds particle corrected for the porosity [−]
$Re_{\varepsilon,mf}$	Reynolds corrected for the porosity at minimum fluidisation [−]
r	Pearson correlation coefficient
rel.error	Error divided by average value [−]
t	Time [s]
T	Temperature [°C]
v_p	Particle phase velocity [m/s]
v_s	Linear superficial velocity or empty tube fluidisation velocity [m/s]
v_t	Terminal particle settling velocity [m/s]
v_E	Apparent free-falling settling velocity of a particle in an infinite dilution [m/s]
V	Volume [m^3]
x	Average particle diameter between top and bottom sieves [m]

Greek symbols

α, β	Coefficients [−]
ε	Porosity or voidage of the system [m^3/m^3]
ε_o	Fixed bed porosity [−]
η	Dynamic fluid viscosity [kg/m/s]
ε_{mf}	Porosity at minimum fluidisation [−]
κ, λ	Coefficients [−]
μ	Statistical mean
ρ_c	Density of calcium carbonate [kg/m^3]
ρ_f	Fluid density [kg/m^3]
ρ_g	Seeding material density [kg/m^3]
ρ_p	Particle density [kg/m^3]
σ	Standard deviation
ϕ_S	Sphericity, shape of diameter correction factor [−]

Subscripts, superscripts and abbreviations

0	Fixed bed state
ARE	Average relative error
BL	Brown-Lawler
c	Calcium carbonate $CaCO_3$
calc	Calculated value
CK	Carman-Kozeny
EG	Ergun
exp.	Experimental value
f	Fluid properties
i	Index number
g	Garnet
KZ	Kozeny
LW	Lewis
max	Maximum
mf	Minimal fluidisation conditions
p	Particle properties
ref.	Reference value

t	Terminal settling conditions
tot	Total or overall
TDS	Total dissolved solids

Acknowledgements

This research is part of the project "Hydraulic modelling of liquid-solid fluidisation in drinking water treatment processes" carried out by Waternet, Delft University of Technology and HU University of Applied Sciences Utrecht. Financial support came from Waternet's Drinking Water Production Department. This research did not receive any specific grant from funding agencies in the public, commercial, or not-for-profit sectors.

Appendix A. Supplementary data

Supplementary data to this article can be found online at https://doi.org/10.1016/j.powtec.2018.11.018.

References

[1] A. Graveland, J.C. van Dijk, P.J. de Moel, J.H.C.M. Oomen, Developments in water softening by means of pellet reactors, J. AWWA - Am. Water Work. Assoc. (1983) 619–625.
[2] J.E. Amburgey, Optimization of the extended terminal subfluidization wash (ETSW) filter backwashing procedure, Water Res. 39 (2005) 314–330, https://doi.org/10.1016/j.watres.2004.09.020.
[3] J.A.M.H. Hofman, O.J.I. Kramer, J.P. van der Hoek, M.M. Nederlof, M. Groenendijk, Twenty years of experience with central softening in the Netherlands, water quality, environmental benefits and costs, Water 21, Int. Symp. Heal. Asp. Calcium Magnes. Drink. Water, Washington, DC 2007, pp. 1–8.
[4] J.C. van Dijk, D.A. Wilms, Water treatment without waste material-fundamentals and state of the art of pellet softening, J. Water Supply: Res. Technol. AQUA 40 (1991) 263–280.
[5] K.M. van Schagen, L.C. Rietveld, R. Babuška, O.J.I. Kramer, Model-based operational constraints for fluidised bed crystallisation, Water Res. 42 (2008) 327–337, https://doi.org/10.1016/j.watres.2007.07.019.
[6] K.M. van Schagen, L.C. Rietveld, R. Babuška, E.T. Baars, Control of the fluidised bed in the pellet softening process, Chem. Eng. Sci. 63 (2008) 1390–1400, https://doi.org/10.1016/j.ces.2007.07.027.
[7] M.J.A. Schetters, J.P. van der Hoek, O.J.I. Kramer, L.J. Kors, L.J. Palmen, B. Hofs, H. Koppers, Circular economy in drinking water treatment: reuse of ground pellets as seeding material in the pellet softening process, Water Sci. Technol. 71 (2015) 479–486, https://doi.org/10.2166/wst.2014.494.
[8] L.J. Palmen, M.J.A. Schetters, J.P. van der Hoek, O.J.I. Kramer, L.J. Kors, B. Hofs, H. Koppers, Circular economy in drinking water treatment: re-use of grinded pellets as seeding material in the pellet softening process, IWA World Water Congr. Exhib. Lisbon, Lisbon 2014, p. 1.
[9] M. Asif, Generalized Richardson-Zaki correlation for liquid fluidization of binary solids, Chem. Eng. Technol. 21 (1998) 77–82, https://doi.org/10.1002/(SICI)1521-4125(199801)21:1<77::AID-CEAT77>3.0.CO;2-#.
[10] O. Akgiray, E. Soyer, An evaluation of expansion equations for fluidized solid-liquid systems, J. Water Supply Res. Technol. - AQUA. 55 (2006) 517–525, https://doi.org/10.2166/aqua.2006.040.
[11] S. Slaa, D.S. van Maren, J.C. Winterwerp, On the Hindered Settling of Silt-Water Mixtures, 4th Int. Conf. Estuaries Coasts, 8–11 Oct. 2012, Water Resour. Univ. Vietnam 2012, pp. 1–13.
[12] M. Đuriš, T.K. Radoičić, Z. Arsenijević, R. Garić-Grulović, Ž. Grbavčić, Prediction of bed expansion of polydisperse quartz sand mixtures fluidized with water, Powder Technol. 289 (2016) 95–103, https://doi.org/10.1016/j.powtec.2015.11.047.
[13] J.F. Richardson, W.N. Zaki, Sedimentation and fluidisation: part I, Trans. Inst. Chem. Eng. 32 (1954) 35–53, https://doi.org/10.1016/S0263-8762(97)80006-8.
[14] R. Darby, R.P. Chhabra, Chemical Engineering Fluid Mechanics, 2nd ed. Marcel Dekker Inc, New York, 2001.
[15] A.H. Dharmarajah, Effect of Particle Shape on Prediction of Velocity-Voidage Relationship in Fluidized Solid-Liquid Systems, 1982.
[16] C.K. Gupta, D. Sathiyamoorthy, Fluid Bed Technology in Materials Processing, 1st ed. CRC Press LLC., Florida, 1999http://books.google.com/books?id=pnwsQb1WPqwC&pgis=1.
[17] J. Li, M. Kwauk, Particle-Fluid Two-Phase Flow: The Energy-Minimization Multi-Scale Method, Metallurgical Industry Press, Beijing, 1994.
[18] L.G. Gibilaro, Fluidization-Dynamics, the Formulation and Applications of a Predictive Theory for the Fluidized State, Butterworth-Heinemann, Oxford, 2001.
[19] R.G. Holdich, Fundamentals of Particle Technology, Midland Information Technology and Publishing, Leicestershire, 2002https://doi.org/10.4236/ns.2010.210132.
[20] W.C. Yang, Handbook of Fluidization and Fluid-particle Systems, 1st ed. CRC Press, New-York, 2003https://doi.org/10.1016/S1672-2515(07)60126-2.
[21] S. Oka, E.J. Anthony, Fluidized Bed Combustion, CRC Press, New-York, 2003https://doi.org/10.1201/9781420028454.ch2.
[22] S.M. Peker, B. Helvaci, B. Yener, A. Alparslan Ikizler, Solid-Liquid Two Phase Flow, Elsevier Science, 2008https://doi.org/10.1016/B978-0-444-52237-5.X5001-2.
[23] J.G. Yates, Fundamentals of Fluidized-Bed Chemical Processes, Butterworth-Heinemann, London, 1983http://www.sciencedirect.com/science/article/pii/B9780408709095500126.
[24] J.G. Yates, P. Lettieri, Fluidized-Bed Reactors: Processes and Operating Conditions, Springer International Publishing, 2016https://doi.org/10.1007/978-3-319-39593-7.
[25] M. Rhodes, Introduction to Particle Technology, 2nd ed. John Wiley & Sons Ltd, Chichester, 2008https://doi.org/10.1002/9780470727102.
[26] J.P.K. Seville, C.Y. Yu, Particle Technology and Engineering, an engineer's Guide to Particles and Powders: Fundamentals and Computational Approaches, 1st ed. Butterworth-Heinemann, 2016.
[27] C.T. Crowe, F. Group, Multiphase Flow Handbook, 1st ed. CRC Press, 2006.
[28] J.M. Coulson, J.F. Richardson, Coulson Richardson Chemical Engineering (Volume 2), 3rd ed. Pergamon Press, 1957.
[29] J.H. Harker, J.R. Backhurst, J.F. Richardson, Coulson & Richardson's Chemical Engineering, 5th ed.Vol. 2, Butterworth-Heinemann, 2002.
[30] A. Busciglio, Measurement Techniques and Modelling of Multiphase Systems, Universitá degli Studi di Palermo, 2011.
[31] A.R. Khan, J.F. Richardson, Fluid-particle interactions and flow characteristics of fluidized beds and settling suspensions of spherical particles, Chem. Eng. Commun. 78 (1989) 111–130, https://doi.org/10.1080/00986448908940189.
[32] J.F. Richardson, W.N. Zaki, Sedimentation and fluidisation. Part I, this week's citation classic, Trans. Inst. Chem. Eng. 32 (1979) 35–53.
[33] T. Siwiec, The experimental verification of Richardson-Zaki law on example of selected beds used in water treatment, Electron. J. Polish Agric. Univ. Ser. Civ. Eng. 10 (2007) 72–76.
[34] J. Garside, M.R. Al-Dibouni, Velocity-voidage relationships for fluidization and sedimentation in solid-liquid systems, Ind. Eng. Chem. Process. Des. Dev. 16 (1977) 206–214, https://doi.org/10.1021/i260062a008.
[35] P.N. Rowe, A convenient empirical equation for estimation of the Richardson-Zaki exponent, Chem. Eng. Sci. 43 (1987) 2795–2796, https://doi.org/10.1016/0009-2509(87)87035-5.
[36] A.R. Khan, J.F. Richardson, The resistance to motion of a solid sphere in a fluid, Chem. Eng. Commun. 62 (1987) 135–150, https://doi.org/10.1080/00986448708912056.
[37] W.K. Lewis, E.R. Gilliland, W.C. Bauer, Characteristics of fluidized particles, Ind. Eng. Chem. 41 (1949) 1104–1117, https://doi.org/10.1021/ie50474a004.
[38] A.D. Maude, R.L. Whitmore, A generalized theory of sedimentation, Br. J. Appl. Phys. 9 (1958) 477–482, https://doi.org/10.1103/RevModPhys.20.35.
[39] J.F. Richardson, M.A. da S. Jerónimo, Velocity-voidage relations for sedimentation and fluidisation, Chem. Eng. Sci. 34 (1979) 1419–1422, https://doi.org/10.1016/0009-2509(79)85167-2.
[40] R. Clift, J.R. Grace, M.E. Weber, Bubbles, Drops, and Particles, Academic Press, San Diego, San Diego, C.A., 1978
[41] R. Di Felice, Review article number 47: of hydrodynamics of liquid fluidisation, Chem. Eng. Sci. 50 (1995) 1213–1245, https://doi.org/10.1016/0009-2509(95)98838-6.
[42] D. Pal, K. Ghoshal, Hindered settling with an apparent particle diameter concept, Adv. Water Resour. 60 (2013) 178–187, https://doi.org/10.1016/j.advwatres.2013.08.003.
[43] R. Di Felice, L.G. Gibilaro, Wall effects for the pressure drop in fixed beds, Chem. Eng. Sci. 59 (2004) 3037–3040, https://doi.org/10.1016/j.ces.2004.03.030.
[44] M. Bargieł, E.M. Tory, Extension of the Richardson-Zaki equation to suspensions of multisized irregular particles, Int. J. Miner. Process. 120 (2013) 22–25, https://doi.org/10.1016/j.minpro.2013.02.011.
[45] S. Schiaffino, H.K. Kytömaa, Steady fluidization of fine particles in a fixed bed of coarse particles, Powder Technol. 77 (1993) 291–299, https://doi.org/10.1016/0032-5910(93)85021-Z.
[46] P. Glasserman, D. Videla, U. Böhm, Liquid fluidization of particles in packed beds, Powder Technol. 79 (1994) 237–245, https://doi.org/10.1016/0032-5910(94)02822-2.
[47] J. Yang, A. Renken, A generalized correlation for equilibrium of forces in liquid-solid fluidized beds, Chem. Eng. J. 92 (2003) 7–14, https://doi.org/10.1016/S1385-8947(02)00084-0.
[48] J.M. Valverde, A. Castellanos, A modified Richardson-Zaki equation for fluidization of Geldart B magnetic particles, Powder Technol. 181 (2008) 347–350, https://doi.org/10.1016/j.powtec.2007.05.018.
[49] C.E. Capes, Particle agglomeration and the value of the exponent n in the Richardson-Zaki equation, Powder Technol. 10 (1974) 303–306, https://doi.org/10.1016/0032-5910(74)85005-9.
[50] Y.S. Chong, D.A. Ratkowsky, N. Epstein, Effect of particle shape on hindered settling in creeping flow, Powder Technol. 23 (1979) 55–66, https://doi.org/10.1016/0032-5910(79)85025-1.
[51] M. Johnson, J. Peakall, M. Fairweather, S. Biggs, D. Harbottle, T.N. Hunter, Characterization of multiple hindered settling regimes in aggregated mineral suspensions, Ind. Eng. Chem. Res. 55 (2016) 9983–9993, https://doi.org/10.1021/acs.iecr.6b02383.
[52] R. Di Felice, M. Rotondi, Solid suspension by an upflow mixture of fluid and larger particles, Adv. Mech. Eng. (2013) 2013, https://doi.org/10.1155/2013/859756.
[53] R. Girimonte, V. Vivacqua, The expansion process of particle beds fluidized in the voids of a packing of coarse spheres, Powder Technol. 213 (2011) 63–69, https://doi.org/10.1016/j.powtec.2011.07.006.
[54] R. Girimonte, V. Vivacqua, Design criteria for homogeneous fluidization of Geldart's class b solids upward through a packed bed, Powder Technol. 249 (2013) 316–322, https://doi.org/10.1016/j.powtec.2013.08.041.

[55] M. Đuriš, R. Garić-Grulović, Z. Arsenijević, D. Jaćimovski, Ž. Grbavčić, Segregation in water fluidized beds of sand particles, Powder Technol. 235 (2013) 173–179, https://doi.org/10.1016/j.powtec.2012.10.004.
[56] M.R. Tomkins, T.E. Baldock, P. Nielsen, Hindered settling of sand grains, Sedimentology 52 (2005) 1425–1432, https://doi.org/10.1111/j.1365-3091.2005.00750.x.
[57] T.E. Baldock, M.R. Tomkins, P. Nielsen, M.G. Hughes, Settling velocity of sediments at high concentrations, Coast. Eng. 51 (2004) 91–100, https://doi.org/10.1016/j.coastaleng.2003.12.004.
[58] H. Yang, M. Fan, A. Liu, L. Dong, General formulas for drag coefficient and settling velocity of sphere based on theoretical law, Int. J. Min. Sci. Technol. 25 (2015) 219–223, https://doi.org/10.1016/j.ijmst.2015.02.009.
[59] R. Barati, S.A.A.S. Neyshabouri, G. Ahmadi, Development of empirical models with high accuracy for estimation of drag coefficient of flow around a smooth sphere: an evolutionary approach, Powder Technol. 257 (2014) 11–19, https://doi.org/10.1016/j.powtec.2014.02.045.
[60] N.S. Cheng, Comparison of formulas for drag coefficient and settling velocity of spherical particles, Powder Technol. 189 (2009) 395–398, https://doi.org/10.1016/j.powtec.2008.07.006.
[61] L.G. Gibilaro, R. Di Felice, S.P. Waldram, P.U. Foscolo, Generalized friction factor and drag coefficient correlations for fluid particle interactions, Chem. Eng. Sci. 40 (1985) 1817–1823.
[62] J.K. Edzwald, Water quality & treatment: a handbook on drinking water, 6th ed. American Water Works Association, American Society of Civil Engineers, McGraw-Hill, New York, 2011.
[63] O.J.I. Kramer, P.J. de Moel, E.T. Baars, W.H. van Vugt, J.P. van der Hoek, Prediction of the Terminal Settling Velocity of Natural Particles Applied in Drinking Water Treatment Processes - ARTICLE UNDER REVIEW, 2018 1–19.
[64] P.P. Brown, D.F. Lawler, Sphere drag and settling velocity revisited, J. Environ. Eng. 129 (2003) 222–231, https://doi.org/10.1061/(ASCE)0733-9372(2003)129:3(222.
[65] L. Schiller, A. Naumann, Über die grundlegenden berechnungen bei der schwerkraftaufbereitung, Zeitschrift Des Vereines Dtsch. Ingenieure. 29 (1933) 318–320.
[66] J. Kozeny, Über kapillare leitung des wassers im boden, Akad. Wiss.Wien. 136 (1927) 271–306.
[67] P.C. Carman, Fluid flow through granular beds, Trans. Inst. Chem. Eng. 15 (1937) 32–48, https://doi.org/10.1016/S0263-8762(97)80003-2.
[68] P. Forchheimer, Wasserbewegung durch boden, Zeitschrift Des Vereines Dtsch. Ingenieuer. 45 (1901) 1781–1788.
[69] J. Happel, N. Epstein, Cubical assemblages of uniform spheres, Ind. Eng. Chem. 46 (1954) 1187–1194, https://doi.org/10.1021/ie50534a033.
[70] S. Ergun, Fluid flow through packed columns, Chem. Eng. Sci. 48 (1952) 89–94 (doi: citeulike-article-id:7797897).
[71] W.K. Lewis, E.R. Gilliland, P.M. Lang, Entrainment from fluidized beds, Chem. Eng. Prog. Symp. Ser. 58 (1962) 65–78.
[72] M.M. Clark, Transport Modeling for Environmental Engineers and Scientists, 2nd ed. John Wiley & Sons Ltd, New York, 2009.
[73] D. Kunii, D. Levenspiel, Fluidization engineering, 1st ed. Robert E. Krieger Publishing Co. John Wiley and Sons, 1969.
[74] O.J.I. Kramer, M.A. Jobse, E.T. Baars, A.W.C. van der Helm, M.G. Colin, L.J. Kors, W.H. van Vugt, Model-based prediction of fluid bed state in full-scale drinking water pellet softening reactors, IWA Congr. New Dev. It Water Conf 2015, pp. 1–26.
[75] N.E.N.-E.N. 933-2, Tests for Geometrical Properties of Aggregates - Part 2: Determination of Particle Size Distribution - Test Sieves, Nominal Sizes of Apertures, Dutch norm, ICS-code 91.100.15, 93.080.20 1996.
[76] D. Geldart, Estimation of basic particle properties for use in fluid-particle process calculations, Powder Technol. 60 (1990) 1–13, https://doi.org/10.1016/0032-5910(90)80099-K.
[77] J.W. Anthony, R.A. Bideaux, K.W. Bladh, M.C. Nichols, "Calcite, Handbook of Mineralogy", V, Borates, Carbonates, Sulfates, Mineral Data Publishing, 1st ed. Mineralogical Society of America, 2003.
[78] W.M. Haynes, Handbook of Chemistry and Physics, 96th ed. CRC Press, 2017.
[79] R.H. Perry, D.W. Green, Perry's Chemical engineers' Handbook, 50th ed. McGraw-Hill Int, 2007.
[80] J. Albright, Albright's Chemical Engineering Handbook, 1st ed. CRC Press, New-York, 2009.
[81] H. Vogel, Das temperatur-abhängigkeitsgesetz der viskosität von flüssigkeiten, Zeitschrift Für Phys. 22 (1921) 645–646.
[82] F. Civan, Critical modification to the Vogel-Tammann-Fulcher equation for temperature effect on the density of water, Ind. Eng. Chem. Res. 46 (2007) 5810–5814, https://doi.org/10.1021/ie070714j.
[83] M.H. Sharqawy, V.J.H. Lienhard, S.M. Zubair, The thermophysical properties of seawater: a review of existing correlations and data accessed thermophysical properties of seawater: a review of existing correlations and data, Desalin. Water Treat. 16 (2010) 354–380, https://doi.org/10.5004/dwt.2010.1079.
[84] A. Haider, O. Levenspiel, Drag coefficients and terminal velocity of spherical and nonspherical particles, Powder Technol. 58 (1989) 63–70.
[85] C.Y. Wen, Y.H. Yu, A generalized method for predicting the minimum fluidization velocity, Am. Inst. Chem. Eng. J. 12 (1966) 610–612, https://doi.org/10.1002/aic.690120343.
[86] G.B. Wallis, One Dimensional Two Phase Flow, McGraw-Hill Int, 1969.
[87] K.M. van Schagen, Model-Based Control of Drinking-Water Treatment Plants, http://repository.tudelft.nl/view/ir/uuid%3Afc4d865d-1ed7-409e-83ba-6270dacdec67/ 2009.